

ОБЪЕДИНЕННЫЙ
ИНСТИТУТ
ЯДЕРНЫХ
ИССЛЕДОВАНИЙ

Дубна

E7-96-364

A.N.Andreyev, D.D.Bogdanov, V.I.Chepigin,
A.P.Kabachenko, O.N.Malyshev, Yu.A.Muzychka,
Yu.Ts.Oganessian, A.G.Popeko, B.I.Pustyl'nik, R.N.Sagaidak,
G.M.Ter-Akopian, A.V.Yeremin

DECAY WIDTHS
OF HIGHLY EXCITED Ra COMPOUND NUCLEI

Submitted to «Nuclear Physics A»

1996

Ширины распада высоковозбужденных компаунд ядер Ra

Для компаунд ядер $^{216,218,220}\text{Ra}$, полученных в реакциях $^{22}\text{Ne} + ^{194,196,198}\text{Pt}$, были измерены функции возбуждения для xn , pxn и αxn -каналов распада в области энергий возбуждения от 40 МэВ до 130 МэВ. За счет использования реакций на трех изотопах платины, в работе с хорошей степенью точности были измерены отношения сечений испарительных реакций, приводящих к образованию одного и того же конечного ядра, но с различным числом ступеней в испарительном каскаде, что позволило определить экспериментальные величины приведенных нейтронных ширин при высоких энергиях возбуждения компаунд ядра.

Установлено, что во всем диапазоне энергий возбуждения сечения образования испарительных продуктов в реакциях $^{22}\text{Ne} + ^{194,196,198}\text{Pt}$ хорошо описываются в рамках статистической модели испарения с учетом оболочечных поправок по Игнатьюку. Как показывают наши настоящие и предыдущие исследования, использование такого подхода позволяет с одним набором модельных параметров ($C = 0.6 - 0.7$ и $\bar{\alpha}_f/\bar{\alpha}_v \leq 1.00$) правильно описывать величины сечений образования испарительных продуктов в широкой области компаунд ядер — от Bi до U.

Работа выполнена в Лаборатории ядерных реакций им.Г.Н.Флерова ОИЯИ.

Препринт Объединенного института ядерных исследований. Дубна, 1996

Andreyev A.N. et al.

E7-96-364

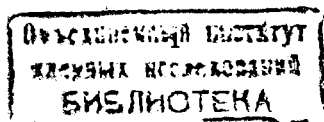
Decay Widths of Highly Excited Ra Compound Nuclei

Excitation functions were measured for the xn , pxn and αxn decay channels of the compound nuclei of $^{216,218,220}\text{Ra}$ produced in the reactions $^{22}\text{Ne} + ^{194,196,198}\text{Pt}$ in the excitation energy range of 40 – 160 MeV. Due to the employment of three platinum isotope targets the cross-section ratios have been measured with a high degree of accuracy for reactions leading to the same final products after termination of evaporation cascades involving different numbers of stages. It is shown that the evaporation reaction cross-sections are well described in the framework of the statistical model taking into account shell effects according to Ignatyuk. Our present, and also earlier, investigations show that such calculations making use of one single set of the model parameters — the scaling factor to the liquid-drop barrier of Cohen, Plasil and Swiatecki $C = 0.6 - 0.7$ and the ratio of the level density parameters $\bar{\alpha}_f/\bar{\alpha}_v \leq 1.00$ — reproduce correctly cross-sections of evaporation reactions in a wide range of compound nuclei extending from Bi to U.

The investigation has been performed at the Flerov Laboratory of Nuclear Reactions, JINR.

1. Introduction

Reactions between complex nuclei succeeding in the compound nucleus formation are suitable for the investigation of both the thermodynamical characteristics of nuclear matter (temperature of hot nuclei and decay widths) as well as its dynamical characteristics (the rate of the energy dissipation, viscosity, etc.). Usually, the relevant investigations make use of experimental data as trials allowing to obtain the values of the model parameters introduced in the framework of one or another theoretical approach to the problems of the compound nucleus formation and its de-excitation and see how these parameters are varied in dependence of the experimentally controlled conditions – such as the nucleus excitation energy, transferred momentum, entrance channel mass asymmetry, etc. The large body of data obtained during the last several years for the number of pre-fission neutrons emitted in heavy-ion reactions stimulated a lively discussion about the mechanism of the neutron emission and origin of the fission width of hot compound nuclei [1,2]. One of the problems discussed is related to the finding that the experimentally observed number of pre-fission neutrons is larger than that which follows from statistical model calculations, and this difference tends to increase with growing excitation energy. In order to give an explanation to this difference, new approaches were suggested where the fission width was calculated by making use of formulae taking into account nuclear viscosity [3,4]. It appears to us, however, that when discussing the discrepancy between the experimental data and statistical model calculations the well known detail is underestimated and that the fitting of the calculated results to the measured integral fission cross-section does not impose a considerable limitation to the calculated number of pre-fission neutrons. For example, it was shown [5,6] that a correlated variation of the model parameters responsible for the nuclear level density and liquid-drop fission barrier allows, keeping up a satisfactory fit of fission excitation functions, to increase the $\langle \nu_{pre} \rangle$ by a factor of 2.5 as compared to the estimation assuming generally adopted values of these parameters. This does



not seem to be surprising since the value of $\langle \nu_{pre} \rangle$ is very sensitive to the values of Γ_n/Γ_{tot} for the initial steps of de-excitation cascade, whereas the total fission cross section depends also on other model parameters. Therefore the issue of the correctness of the parameters which are used in statistical model calculations becomes imperative when one is involved into the interpretation of experimental data on formation and de-excitation of heavy compound nuclei. It appears to us that, before working out a new dynamical approach to the fission of highly excited compound nuclei and fitting the model parameters, it is necessary to clearly identify the experimental data which really can not be described in the framework of the standard statistical model assuming a minimum set of requirements to the de-excitation process, namely, that the compound nucleus is perfectly equilibrated, and the relative probabilities of the nucleus different decay channels are governed by their statistical weights defined in the phase space of the system.

The present work is a continuation of our study of formation cross sections of evaporation residues which are obtained in heavy ion complete fusion reactions leading to compound nuclei in the region extending from Bi to U [7-9]. We measured excitation functions of the xn, pxn and α xn decay channels in the excitation energy range of 40-160 MeV of the compound nuclei of $^{216,218,220}\text{Ra}$ produced in the reactions $^{22}\text{Ne} + ^{194,196,198}\text{Pt}$. Our interest to these reactions arouse because some information can be obtained about the role of shell effects in the decay of highly excited Ra compound nuclei. On the other hand we were interested to see to what extent can the statistical model describe in a wide range of excitation energy the decay width ratios including also the fission width and the numbers of pre-fission (more precisely – pre-saddle) particles. The use of the reactions occurring with three platinum isotopes allowed us to measure, with a good precision, the cross section ratios for reactions leading to the formation of individual evaporation residues after evaporation of different numbers of neutrons. Knowledge of these ratios allowed us to impose an essential and, as it will be shown later, stringent

condition which should be satisfied by a model assumed to correctly fit the evaporation residue cross sections and give a direct information on the fissility of the compound nucleus at the initial stages of evaporation cascade. We discussed earlier some preliminary data of these experiments [10,11].

2. Experimental method

The experiments were carried out at the beam of the U-400 cyclotron (Flerov Laboratory of Nuclear Reactions, JINR). The cyclotron provided the beams of ^{22}Ne of five discrete energy values – 135, 160, 176, 192 and 225 MeV. The beam energy was varied with steps of 3-6 MeV by making use of Al and Ti degraders. The intensity of the beam passed through the target was measured by means of Faraday cap. It was limited at the level of $2 \times 10^{11} \text{ s}^{-1}$. Targets of the enriched isotopes of $^{194,196,198}\text{Pt}$ deposited on thin (0.4 mg/cm^2) aluminum backings were used in the experiments. The target isotopic compositions are presented in Table 1. The thickness of each target

Table 1. Isotopic compositions and thicknesses of targets

Target	Thickness mg/cm ²	Isotopic composition, %			
		194	195	196	198
^{194}Pt	165	83.0	13.0	3.5	0.5
^{196}Pt	315	2.3	7.1	86.8	3.8
^{198}Pt	250	3.7	4.9	5.6	85.7

was measured by the X ray fluorescent analysis just after manufacture and after the completion of the experiments. The results of the measurements were reproduced well, and the precision of $\pm 5\%$ and $\pm 15\%$ was estimated, respectively, for the measurements of relative and absolute values of the target thicknesses.

The bombarding ion energy was measured with a Si detector that was hit by ions scattered from the target at 30° . The detector was calibrated with standard α -sources. The non-ionization energy loss and the loss of energy in the "dead" surface layer of the detector were

not taken into account. According to our estimations, the accuracy of such an approach to the energy measurement makes $\pm(1.0-1.5)\%$ for $A \leq 40$ ions. For our experiments, this implied the absolute value of the error of ± 2.5 MeV in the measurements of the ion energy.

Products of the complete fusion reactions were separated from the bombarding ions and products of transfer and deep inelastic reactions with the aid of the kinematic separator VASSILISSA [12,13]. This is a three stage electrostatic separator providing transmission of reaction products emerging from the target in forward direction within the solid angle of 15 msr and having the electric stiffness within a band of $\pm 10\%$. Evaporation residues of $A > 200$ having the life time of more than $\sim 1 \mu s$ can be delivered to the separator focal plane with the efficiency ranging from 3% (for the case of oxygen bombarding ions) to 25% (for Ar and Ca ions).

Recoil nuclei delivered to the separator focal plane first passed a pair of the broad aperture detectors [14] providing the measurement, with the resolution of 0.5 ns, of the recoil time of flight on the path of 50 cm and then were implanted into an eight-strip Si detector having the active surface of $50 \times 70 \text{ mm}^2$ and providing the energy resolution of 30 keV for α particles in the energy range of 5–9 MeV. The recoil nuclei were identified according to their α -decay energy values and excitation functions. The separator efficiency was measured in these experiments by making use of the reaction $^{22}\text{Ne}(135 \text{ MeV}) + ^{\text{nat}}\text{W}(340 \mu\text{g}/\text{cm}^2)$, and it made $(3.7 \pm 0.5)\%$. We accomplished these measurements of the efficiency [9] by comparing the α -activity obtained in the separator focal plane with that detected in a catcher foil which could be placed just behind the target. Systematic errors in the measurements of the relative cross-section values were minimized by means of carrying out the major part of the experiments within a single bombardment period having a fixed separator tune. At a given beam energy, the measurements were performed successively for each of three targets. The targets were changed by means of a remote control. For each fixed beam energy the mean irradiation time made 25–30 minutes. Between the irradiations,

the long-lived α -activity implanted into the strip detector was measured for 10 minutes. The full energy range of the beam (100–225 MeV) was divided in six intervals with the mean energy values of 126, 108, 145, 167, 185 and 205 MeV, and the irradiations were carried out in these energy intervals in the succession as these are listed here.

3. Experimental data

We obtained the excitation functions of xn, pxn and α xn reactions for the compound nuclei of $^{216,218,220}\text{Ra}$ in the range of excitation energy of 40–160 MeV. The data of our measurements are presented in Tables 2–4.

Experimental mass tables [15] were used in the calculations of the excitation energy values. Alpha decay branching ratios were obtained from Ref. [16]. The treatment of the raw experimental results involved corrections for the background caused by the admixtures of different Pt isotopes in the targets. This background was subtracted taking into account the energy dependencies of the individual α -activity yields obtained for three targets.

As an example, the points for the experimental cross sections obtained for the xn evaporation channels of the reaction $^{22}\text{Ne} + ^{198}\text{Pt}$ are shown in Fig.1 together with the curves calculated with a statistical model. One can see from figure that, in spite of the wide range of the cross section variation, the calculations reproduce well enough both the relative and absolute values of the cross sections. A small discrepancy in the energy positions of the experimental and calculated maximums of the excitation curves is within our accuracy of the beam energy measurements. It can be eliminated by a sole shift of the experimental points by 3–5 MeV to the right side. The calculations will be discussed in more details in the next section.

Maximum values of the formation cross sections are presented in Table 5 for $A=206-214$ Ra isotopes. One can see from this table that the ratios of the maximum cross sections of individual Ra isotopes formed as a result xn and $(x+2)n$ reactions ($\sigma_{xn}/\sigma_{(x+2)n}$) is practically the same in the whole range of the mass numbers, irrespective of the

absolute cross-section value (one can see from Table 5 that the cross section drops down by a factor of 5×10^4 at the transition from ^{212}Ra to ^{206}Ra). Qualitatively, this implies that the partial fission decay width Γ_f is small at the initial stages of the de-excitation cascade, and the fission occurring at this stages does not play an essential role in the formation cross sections of evaporation residues.

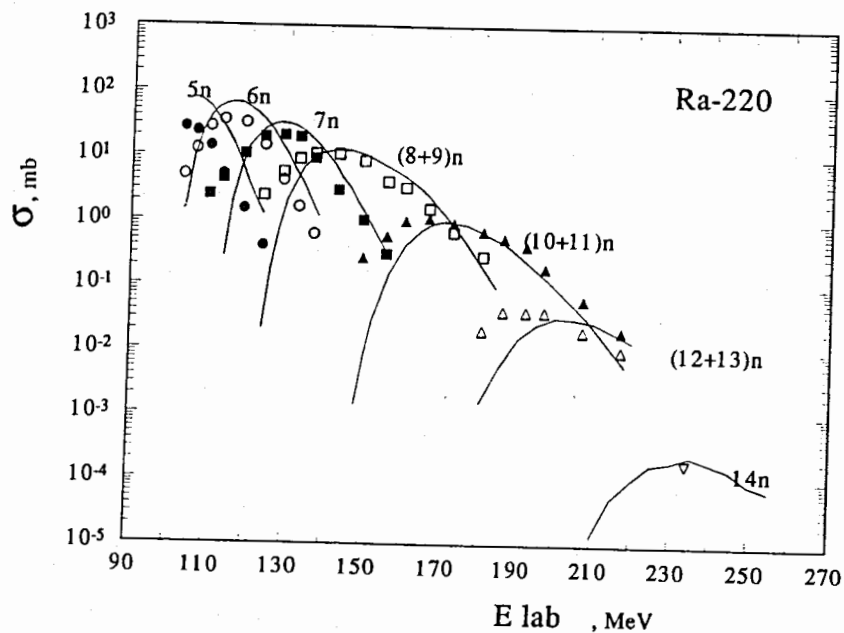


Fig. 1. Excitation curves of xn channels of the reaction $^{22}\text{Ne} + ^{198}\text{Pt}$. Experimental data are shown with symbols; lines show the results of calculations made with the statistical model incorporating shell effects (parameter values are: $C=0.63$, $\bar{a}_f/\bar{a}_\nu=1.00$).

A brief explanation to the data of Table 5 appears to be necessary. For three pairs of isotopes ($^{211}\text{Ra} - ^{212}\text{Ra}$, $^{209}\text{Ra} - ^{210}\text{Ra}$ and $^{207}\text{Ra} - ^{208}\text{Ra}$) the α -decay energies have the differences which are less than 10 keV. Therefore, our Si detector did not allow the separation of the isotopes within these pairs, and, for these pairs, the

Table 2a. Excitation functions of xn-evaporation reactions

		$^{22}\text{Ne} + ^{198}\text{Pt}$				
E_{Ne}	E^*	Cross-Section, mb				
MeV	MeV	5n	6n	7n	8-9n	10-11n
103.5	45.0	27.3	5.0			
106.5	47.5	23.5	12.5			
110.0	51.0	13.8	27.7	2.5		
113.5	54.0	5.1	35.1	4.4		
119.0	59.0	1.5	31.6	10.5		
124.0	63.5	0.4	14.2	19.0	2.4	
129.0	68.0		4.1	20.2	5.5	
133.0	71.5		1.6	18.8	8.7	
137.0	75.0		0.6	9.0	10.5	
143.0	80.5			2.9	10.4	0.25
149.5	86.5			1.0	8.1	0.26
155.5	92.0			0.3	3.9	0.56
160.0	96.0				3.2	0.99
166.0	101.0	<u>12-13n</u>			1.5	1.07
172.5	107.0				0.66	0.93
180.5	114.0	0.02			0.28	0.69
186.0	119.0	0.04			0.20	0.54
192.0	124.5	0.04			0.09	0.41
197.0	129.0	0.04			0.04	0.19
207.0	138.0	0.02			0.02	0.06
217.0	147.0	0.01			0.01	0.02

Table 2b. Excitation functions of xn-evaporation reactions

$^{22}\text{Ne}+^{196}\text{Pt}$						
E_{Ne} MeV	E^* MeV	Cross-Sections, mb				
		4n	5n	6-7n	8-9n	10-11n
103.5	46.0	5.05	18.6	1.7		
106.5	48.5	2.84	23.7	3.2		
110.0	51.5	0.95	19.9	7.6		
113.5	54.5	0.32	12.5	14.0		
119.0	59.5		5.4	18.1	0.3	
124.0	64.0		1.6	14.3	0.4	
129.0	68.5			10.5	0.6	
133.0	72.5			8.6	1.05	
137.0	76.0			5.0	1.4	
143.0	81.5			1.9	1.9	
149.5	87.0			0.5	1.6	0.015
155.5	92.5			0.3	1.0	0.024
160.5	97.0				0.7	0.040
166.0	102.0				0.4	0.056
172.0	107.5				0.2	0.052
180.5	115.0					0.036
184.0	118.0					0.036
196.0	129.0					0.014
206.0	138.0					0.006
215.0	146.0					0.002
225.0	155.0					0.001

Table 3. Excitation functions of pxn- and axn-evaporation reactions

$^{22}\text{Ne}+^{198}\text{Pt}$							
E_{Ne} MeV	E^* MeV	Cross-Section, mb					
		p,5n	p,6n	p,8-9n	p,10-11n	p,12-13n	α 12n
110.0	51.0	0.06					
113.5	54.0	0.14	0.07				
119.0	59.0	0.30	0.11				
124.0	63.5	0.28	0.28				
129.0	68.0	0.19	0.42				
133.0	71.5	0.13	0.84				
137.0	75.0	0.07	0.51	0.09			
143.0	80.5	0.02	0.47	0.36			
149.5	86.5		0.23	1.13			
155.5	92.0		0.08	1.48	0.16		
160.0	96.0			2.19	0.25		
166.0	101.0			2.44	0.42		
172.0	107.0			2.07	0.64		
180.5	114.5			1.74	1.19		
186.0	119.0			1.29	1.35		
192.0	124.5			0.98	1.80	0.11	
197.0	129.0			0.51	1.40	0.12	0.10
207.0	138.0			0.19	0.84	0.22	0.11
217.0	147.0			0.09	0.47	0.28	0.33
227.5	155.5				0.26	0.28	0.66

$^{22}\text{Ne}+^{198}\text{Pt}$							
E_{Ne} MeV	E^* MeV	Cross-Sections, mb					
		p,6-7n	p,8-9n	p,10-11n	p,12n	α ,10n	α ,11n
124.0	64.0	0.36					
129.0	68.5	1.12					
133.0	72.5	1.72					
137.0	76.0	1.36	0.10				
143.0	81.5	1.51	0.20				
149.5	87.0	1.17	0.43				
155.5	92.5	1.08	0.91				
160.5	97.0	0.77	1.07	0.025			
166.0	102.0	0.63	1.14	0.082			
172.0	107.5	0.26	1.02	0.10		0.32	
180.5	115.0		0.83	0.33		0.82	
184.0	118.0		0.72	0.41		1.00	
191.0	124.5		0.35	0.37		1.02	
196.0	129.0		0.32	0.38		1.09	0.07
206.0	138.0		0.18	0.36	0.02	1.01	0.38
215.0	146.0		0.06	0.16	0.03	0.56	0.26
225.0	155.0		0.04	0.11	0.03	0.56	0.26

Table 4. Excitation functions of xn-, pxn- and α xn-evaporation reactions

$^{22}\text{Ne} + ^{194}\text{Pt}$									
E_{Ne} MeV	E^* MeV	Cross-Section, mb							
		4-5n	6-7n	8-9n	p,4-5n	p,6-7n	p,8-9n	$\alpha,8n$	$\alpha,9n$
97.0	41.0	5000							
105.0	48.5	10800			290				
109.0	52.0	10200	300		630				
112.5	55.0	9000	1060		960				
118.0	60.0	4700	2500		1160				
123.0	64.5	1500	3000		1180				
128.5	69.5	400	2400	21	930	310			
132.5	73.0		2300	24	1020	620			
136.0	76.0		1200	35	570	600			
142.0	81.5		620	76	280	760			
148.0	87.0		280	91	230	700	40	340	
156.0	94.0			58	100	540	140	450	
160.0	97.5			43		430	240	670	
163.0	100.5			27		230	230	750	
167.0	104.0			21	p,10n	220	310	1010	
171.0	107.5			14	8	120	280	1010	260
180.0	115.5			6	20	70	300	780	470
184.0	119.5			6	32	40	240	680	420
191.0	125.5				30	140	140	420	300
196.0	130.0				22	100	100	300	190
206.0	139.0				26	60	60		170

Table 5. Formation cross sections (in mb) of radium isotopes with $206 \leq A \leq 214$ obtained in the maximum of excitation curves.

Compound	Evaporation residues, σ					
	^{214}Ra	^{213}Ra	^{212}Ra	^{210}Ra	^{208}Ra	$^{206}\text{Ra}^a$
^{220}Ra	36	22	11	1.1	0.040	0.0002
^{218}Ra		24	18	1.9	0.058	0.0004
^{216}Ra			12	2.8	0.096	0.0007

a) cross sections of ^{206}Ra measured with the statistical errors ± 0.0001 mb

measured excitation curves were for the sum of the corresponding xn and (x+1)n reactions. However, the formation cross sections in their maximums are more than for 90 % due to the xn reactions since the cross section steeply decreases at the transition to a smaller mass number of the reaction product (compare the 6n and 7n excitation curves in Fig.1). This conclusion also follows from an inspection of the compound nucleus excitation energy positions of the maximums of excitation curves. Statistical errors of the yields measured at a fixed beam energy for different nuclei involved mainly inaccuracies in accounting for the smooth background underlying the isolated α lines and contribution from admixtures of other platinum isotopes in the targets. These errors did not exceed $\pm 5\%$. An exclusion were the yield data for ^{208}Ra formed in the reaction $^{22}\text{Ne} + ^{198}\text{Pt}$. For this reaction product formed in the region of the maximum cross section of the 12n evaporation reaction channel a notable background was made by ^{214}Ra having the α -decay energy close to that for ^{208}Ra and produced in the 6n reaction channel. We estimated this background by extrapolating the experimental excitation curve for ^{214}Ra obtained in 6n reaction in the region of the maximum of the 12n excitation curve. The estimated statistical errors in the yields derived for ^{208}Ra make $\pm 25\%$.

The measurement accuracy of the cross sections obtained in the present work was dominated by errors in the measurements of separation efficiency, beam doses and target thicknesses. Taking into ac-

count possible systematical errors in these measurements (the most severe errors were assumed in the beam dose monitoring) we believe that the absolute cross-section values presented in Tables 2-4 are accurate within the error bars of $\pm 40\%$.

The errors of the obtained ratios of the maximum cross section values are considerably smaller due to experimental procedure which excluded for these ratios the errors of the beam dose and separation efficiency. As a result, the errors of the maximum cross-section ratios involved mainly the errors in the knowledge of relative target thicknesses and maximum yields derived from 3-4 experimental points obtained in the maximum vicinity. From the long term experience we know that the results of many individual measurements of the yield made for an evaporation residue in different experiments are reproducible within $\pm 15\%$. Therefore, we concluded that it will be safe, to estimate as $\pm 15\%$ the errors ratios of maximum cross-sections, though we believe that this implies some overestimation of the error. To some extent, the obtained pattern of the cross-section ratios (see Table 6) can be considered as a proof of the correctness of the error bar estimation.

4. Discussion of the obtained results

We will divide this section in three parts. In the first part we will briefly formulate the statistical model and discuss the main calculation parameters. In the second part regularity of the maximum cross sections of the xn, pxn and α xn de-excitation channels of the compound nuclei of $^{216,218,220}\text{Ra}$ will be discussed and compared with a large body of similar data obtained in our earlier experiments for other $A > 200$ compound nuclei. And finally, in the third part of this section fissility of Ra compound nuclei will be analyzed, and, in particular, new data about the fission width of excited nuclei will be derived from the analysis of the maximum cross-section ratios of evaporation reactions.

Compound nucleus decay widths

To analyze the experimental data we employed the statistical model making use of a minimum number of parameters, and there-

fore, a minimum number of physical assumptions. This implies a more general scope of the model application and possibility to have less ambiguous inferences, though these are gained on account of a more crude character of the model. Nuclear level density is the most important ingredient of statistical model calculations. We used for the level density the Fermi-gas expressions (without taking the collective enhancement into account) and made account according Ignatyuk [17] for shell effects in the level density parameter.

$$a_\nu(E^*) = \bar{a}_\nu \{1 + [1 - \exp(-0.054E^*)]\Delta W_\nu(A, Z)/E^*\}, \quad (1)$$

where $\bar{a}_\nu = (0.11A - 6.3 \cdot 10^{-5}A^2)$, E^* - the compound nucleus excitation energy, and $\Delta W_\nu(A, Z)$ - the shell correction to the mass of the nucleus formed after the evaporation of the particle ν (i.e. of a neutron, proton or α -particle). We assumed the fission channel level density parameter \bar{a}_f to be constant (i.e. independent of the excitation energy), and kept it proportional to the asymptotic value \bar{a}_ν of the level density parameter in the particle evaporation channel (this implies the neglect of the shell effect in the nucleus saddle point). Fission barriers of the nuclei of the interest were calculated by the formula

$$B_f(l) = CB_f^{LD}(l) + \Delta W^{exp}, \quad (2)$$

where C - is a free parameter, $B_f^{LD}(l)$ - fission barrier obtained in the rotating liquid drop model of Cohen, Plasil and Swiatecki (CPS) [18], and ΔW^{exp} is a correction to the fission barrier which we took equal to the shell correction to the nucleus ground state. For the nuclei involved in our analysis the shell correction value varies from $\approx 5.5 - 7.6$ MeV for the isotopes of Ra, Fr and Rn having $N=126$ to ≈ 1.5 MeV for the nuclei formed after evaporation of ≈ 10 neutrons. For the fission barrier, we also neglected the small shell correction value in the saddle point.

Calculations of the evaporation widths were performed on the basis of the Weiskopf-Ewing formalism.

$$\Gamma_\nu^l(E) = \frac{(2l+1)(2s_\nu+1)m_\nu}{\pi^2 \rho_c(E_c) \hbar^2} \int_0^{E-E(l)-E_\nu} \rho_\nu(E-E(l)-E_\nu-\epsilon) c\sigma_\nu(\epsilon) d\epsilon, \quad (3)$$

where S_ν , E_ν and m_ν are the spin, binding energy and reduced mass of the particle ν ; σ_ν – the cross section of the reverse reaction of the capture of the particle ν having the energy ϵ . We calculated the capture cross sections by optical model using the parameters suggested in Ref. [19]. The fission width was calculated with the classical Bohr-Wheeler formula

$$\Gamma_f^l(E) = \frac{2l+1}{2\pi\rho_c(E_c)} \int_0^{E-E^{sp}(l)-B_f(l)} \rho_f(E - E^{sp}(l) - B_f(l) - \epsilon) d\epsilon, \quad (4)$$

where $E^{sp}(l)$ is the rotation energy in the nucleus saddle point.

In the approach outlined above essential are two parameters – the ratio of the asymptotic values of the level density parameters in fission and evaporation channels ($\tilde{a}_f/\tilde{a}_\nu$) and the free parameter C in the formula (2) employed for fission barrier. In principle, to carry out calculations of the cross sections for evaporation reactions one should know the compound nucleus formation cross section, and this is related to the problem of knowledge of the values of l_{crit} and Δl – the critical value of angular momentum for the compound nucleus formation and the width of the angular momentum range around l_{crit} where the formation probability of the compound nucleus falls down essentially to zero. However, in the case of a highly fissile compound nucleus practically the whole formation cross section of an evaporation residue, taken in the maximum of its value, originates from the partial waves of $l \leq 40$ [9]. These are well below the value of l_{crit} typical for the fusion reactions of ^{22}Ne ions [20].

The problem of a choice of the optimum values of the parameters $\tilde{a}_f/\tilde{a}_\nu$ and C appears to be more complex because both these parameters strongly affect the fission width. The problem of the choice of the value of $\tilde{a}_f/\tilde{a}_\nu$ was considered in a number of papers dealing with the de-excitation of pre-actinide compound nuclei (e.g., see Ref. [21]). Different model considerations yielded for this parameter values ranging from 0.95 to 1.10, and many authors noted only a weak variation of $\tilde{a}_f/\tilde{a}_\nu$ with mass number. Also, it is worth noting that earlier [7-9], using $\tilde{a}_f/\tilde{a}_\nu \cong 1$ we well reproduced cross sections

of evaporation reactions and fissility in a wide range of compound nuclei extending from Bi to U.

Formation cross sections of evaporation residues

Calculations were performed in two versions assuming different approximations: (a) in a purely liquid-drop approximation we took $\Delta W_\nu(A, Z) = 0$ and $\Delta W^{exp} = 0$ and used the liquid-drop values for the nuclear binding energies; (b) in another version we took into account the shell-effect corrections $\Delta W_\nu(A, Z)$ and ΔW^{exp} occurring, respectively, in the level-density parameter (1) and fission barrier (2).

In Figs.2 a,b,c shown are, in dependence of the evaporation residue neutron number, the experimental cross sections for xn and pxn evaporation reaction channels corresponding to the maximums of the excitation curves measured for the reactions of $^{22}\text{Ne} + ^{194,196,198}\text{Pt}$. Dotted lines show the results of calculations made in the purely liquid-drop approximation taking $\tilde{a}_f/\tilde{a}_\nu = 1$ and $C = 0.9$. Other lines show the results obtained in calculations taking into account the shell effects and made with three different values of the parameter $\tilde{a}_f/\tilde{a}_\nu$: 0.95, 1.00 and 1.05 (are shown, respectively, with dashed, solid and dash-dotted lines). For these three cases the optimum values of the parameter C were found to be, respectively, 0.45, 0.63 and 0.88. One can see from the figures that three from the four of the calculation versions can reproduce the experimental data in a wide range of the compound nucleus excitation energy extending from 40 to 160 MeV (this corresponds to the evaporation from 4 to 14 neutrons from compound nuclei). This implies that the model can not be tested solely on the basis of the measured cross sections for evaporation reactions and an unambiguous choice can not be made simultaneously for two parameters $\tilde{a}_f/\tilde{a}_\nu$ and C , even if such cross sections are available for long sequences of evaporation residues. Therefore we conclude that some other data are necessary to make such an unambiguous choice, i.e. disentangle these two parameters. This will be the discussion subject of the next subsection, and now we will discuss in some more detail the possibility of applications of the purely liquid-drop approximation and the approach taking into account shell effects when

fitting formation cross sections of evaporation residues and decay characteristics of highly excited compound nuclei in the region of $Z = 82 - 92$.

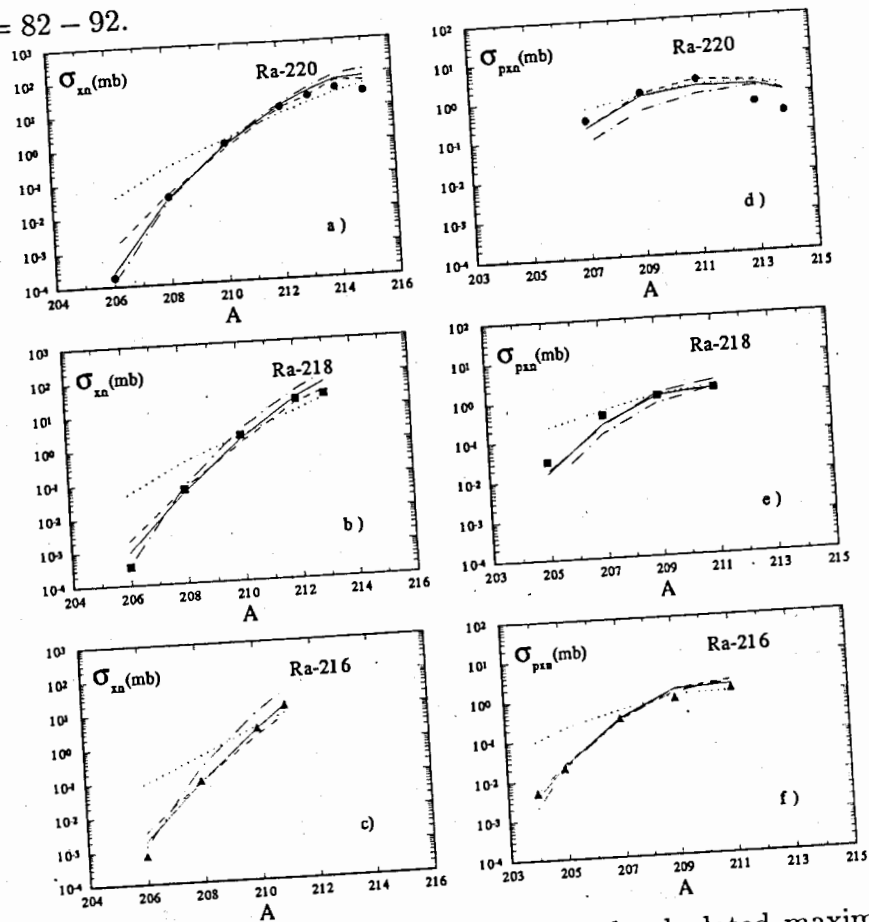


Fig. 2. Comparison of experimental and calculated maximum cross-section values for xn- and pxn de-excitation channels of the compound nuclei formed in the reactions $^{22}\text{Ne} + ^{194,196,198}\text{Pt}$. The results of calculations made in the case of the total neglect of shell effects are shown with dotted lines. Other lines show the results of calculations taking shell effects into account and assuming three different values of the parameter $\bar{a}_f/\bar{a}_\nu = 0.95$ (dashed line), 1.00 (solid line), and 1.05 (dash-dotted line).

The purely liquid-drop approximation was suggested long ago and was widely used in calculations of formation cross sections of evaporation residues of compound nuclei, especially in the transuranium region. The justification of such an approach continues to be the subject of discussions (see e.g. the review paper [22]). In the framework of this discussion an interesting result had been obtained in Ref. [23] where production cross sections were analyzed for $A \approx 200$ neutron-deficient isotopes of astatine and polonium. It was demonstrated in this paper that, at a fixed parameter value \bar{a}_f/\bar{a}_ν , calculations made in two different approximations – one taking the purely liquid-drop formulae and another assuming a synchronous reduction of shell effects in the level density and fission barrier with increasing excitation energy – lead to the essentially coinciding values of the coefficient $C = 0.9 - 1.0$. This implies that the use of the purely liquid-drop approximation is allowable at lower excitation energies for the nuclei having large shell effects, if the shell effects disappear *simultaneously* in the level density and fission barrier with the growing excitation. This gives a strong support in the favour of the liquid-drop approximation when one is interested in calculation of evaporation residue cross sections and allows to consider this approximation as an universal model approach to the situation when the shell effects are rapidly weakened with the growing excitation.

At the same time one can see from Figs.2 that the results of the calculations treating the impact of shell effects within the standard scheme are more favourable in the reproduction of the cross-section patterns. Calculations making use of the liquid-drop approximation give a more weak decrease of cross sections with the grows of neutron deficit then it follows from experiments. This character of discrepancies between the results of calculations and experimental data appears to be typical for the liquid-drop approximation as it was already mentioned in our earlier papers where formation cross sections of neutron-deficient Po, At and Ac isotopes were reported [23-25].

Limitations of the purely liquid-drop approximation become more

evident at an attempt to describe the whole set of data obtained in our experiments for production cross-sections of evaporation residues (ranging from lead to uranium) formed in fusion reactions of heavy ions with $A \leq 40$ (about 15 target-projectile combinations were used to obtain these data). When using this approximation at the fixed value \bar{a}_f/\bar{a}_ν , one is compelled to smoothly increase the parameter C value from 0.65 to 0.9 at the transition from the $N \approx 110$ Bi compound nuclei to the $N \approx 128 - 132$ compound nuclei of Ra-Ac, and then to decrease this parameter steeply to $C = 0.65$ at the transition to the compound nuclei of Pa-U with the neutron numbers of $N \approx 136 - 138$ [24,26]. In other words, by treating the data in the framework of the liquid-drop approximation, one comes to the situation as if the coefficient C "follows" at first the growth of the ground state shell correction from zero (as it is for Bi) to 6 - 8 MeV (for Ra-Ac) and then its decrease to vanishing values at the transition to Pa-U. The need of such a complex variation of the coefficient C for the achievement of an agreement with the experimental data completely eliminates the possibility of use of the liquid-drop approximation for the description of the de-excitation process for compound nuclei lying in this region.

In the light of this observation, it is important that the whole set of data could be fitted very well, with the practically fixed parameters $\bar{a}_f/\bar{a}_\nu = 1$ and $C = 0.63 - 0.70$, in the framework of the outlined calculation version that takes into account the role of the shell effects in the level density and fission barrier. The only assumption that one has to make is that one should decrease by 30 - 40 % the values of the liquid-drop barrier for the nuclei formed in the heavy-ion fusion reactions as compared to the prediction of Cohen-Plasil-Swiatecki [18] or Sierk [27]. One can remind that already in 1978 M.Blann [28] pointed at the necessity to reduce the values of this coefficient up to 0.6-0.7 in order to correctly describe data on fission cross sections of compound nuclei in the region extending from Rh to Os. The lack of reliable experimental data on the fission barriers of neutron-deficient nuclei heavier than Os had led that time to a conclusion that this

effect is specific for lighter fissile nuclei, and it was mirrored in the Sierk model [27]. Now, in the light of the new experimental data which we discuss here, this conclusion loses its justification, and one has to look for a new approach capable to explain the whole data set involving the nuclei from Rh to U.

Arguing for the assumption that values of the liquid-drop barrier should be decreased by 30 - 40 % as compared to the model predictions [18,27] for neutron-deficient nuclei in a wide range of Z we do not exclude that partly this result may be caused by simplifications which we have made. In particular, this effect could emerge from the use of only one single free parameter C in our calculations. However, it appears to be hard to relate to a drawback of the approach the fact that the value of this single parameter appeared to be essentially the same in a wide region of A and Z of the nuclei involved into the evaporation process. Therefore we believe that the matter is not so much in the rough character of the model, but the experimental data lead us to expect that there is the need to look for some general physical reasons that cause the enhanced fissility of these neutron-deficient nuclei. One such attempt was made in Refs. [8,29] where a new formula was suggested and analyzed for the isospin dependence of the liquid-drop barrier. Another possible explanation of the enhanced fissility could be the assumption that the ratio of the asymptotical level-density parameters in the fission and particle evaporation channels of the compound nuclei (\bar{a}_f/\bar{a}_ν) is > 1 . Indeed, it is evident from Figs. 2 that by assuming this ratio to be 1.05 one could come to the value of $C = 0.88$. This possibility we will analyze in the next section.

Neutron widths and fission times of highly excited compound nuclei

Let us come back to Figs.2 a,b,c where experimental cross-section values of xn- and pxn-channels of the reactions $^{22}\text{Ne} + ^{194,196,198}\text{Pt}$ are compared to the calculation results obtained with three parameter sets:

a) $\bar{a}_f/\bar{a}_\nu = 0.95$; $C = 0.45$,

b) $\bar{a}_f/\bar{a}_\nu = 1.00$; $C = 0.63$,

c) $\tilde{a}_f/\tilde{a}_\nu = 1.05$; $C = 0.88$.

One can see, that for these three parameter sets, calculation curves are in a good agreement with experiment, at least these curves keep within the standard error bars of the experimental points. As we mentioned above, two statistical model parameters C and $\tilde{a}_f/\tilde{a}_\nu$ control the nuclear fissility, and small variations of these parameters are crucial for yields of evaporation residues. Yet, as one can see from Figs.2 a properly chosen correlated variation of these parameters allows to come to equally good fits of experimental points for different parameter sets. Therefore to test separately different values of the parameters C and $\tilde{a}_f/\tilde{a}_\nu$ some additional data are necessary.

One such type of data suitable for testing can be the set of data on the reduced widths $\langle \Gamma_n/\Gamma_{tot} \rangle$. One can derive such a reduced width from the ratio of two cross sections measured for one evaporation residue formed after de-excitation of two different compound nuclei. This becomes possible because the fissility of a compound nucleus behaves differently at various excitation energies in dependence of these two parameters. The ratio $\tilde{a}_f/\tilde{a}_\nu$ governs the nuclear fissility mostly at higher excitation energy and defines the number of fission chances, whereas the influence of the parameter C is important at lower excitation energies, more close to the fission barrier.

In Fig.3a shown are calculated ratios $\langle \Gamma_n/\Gamma_{tot} \rangle$ averaged over the partial waves l obtained for the first stage of the evaporation cascade of the ^{220}Ra compound nucleus. These ratios were calculated for three different values of the parameter $\tilde{a}_f/\tilde{a}_\nu$. The averaging is carried out within the angular momentum range of $l = 0 - 40$ since higher partial waves do not play any role when one considers the maximum of the excitation curve for an evaporation residue. Besides, the l dependence of the $\langle \Gamma_n/\Gamma_{tot} \rangle$ is weak in this range; one can note that the extension of the range of averaging up to the critical partial wave $l_{crit} \approx 70$ leads to a decrease of the ratio $\langle \Gamma_n/\Gamma_{tot} \rangle$ only by a factor of 1.5. In this figure shown are also the values of $\langle \Gamma_n/\Gamma_{tot} \rangle$ deduced from our data on the maximum yields of the evaporation residues obtained from the compound nuclei of $^{218,220}\text{Ra}$.

We evaluated these experimental values of $\langle \Gamma_n/\Gamma_{tot} \rangle$ by making use of ratios of the measured maximum formation cross sections of the evaporation residues ^{A-x}Z obtained after evaporation of x and $x+2$ neutrons from two different compound nuclei relatively shifted by two mass units:

$$\frac{\sigma_{(x+2)n}}{\sigma_{xn}} \cong \left[\frac{\sigma_{CN}(x+2)n}{\sigma_{CN}(xn)} \right] \cdot \left\langle \frac{\Gamma_n}{\Gamma_{tot}} \right\rangle_A^2, \quad (5)$$

where $\sigma_{CN}(x+2)n$ and $\sigma_{CN}(xn)$ are the complete fusion cross sections for the bombarding ion energies corresponding, respectively, to the maximum cross sections of $(x+2)n$ and xn evaporation reactions; $\left\langle \frac{\Gamma_n}{\Gamma_{tot}} \right\rangle_A^2$ is the mean value of the reduced neutron width of the compound nucleus AZ having the excitation energy corresponding to the maximum yield of the $(x+2)n$ evaporation reaction.

Table 6. Values of mean reduced neutron widths

	$E^*, \text{M}\text{eV}$	x	$\frac{\sigma_{(x+2)n}}{\sigma_{(xn)}}$	$\frac{\sigma_c(xn)}{\sigma_c(x+2)n}$	$(\Gamma_n/\Gamma_{tot})^2$	Γ_n/Γ_{tot}
$^{220}\text{Ra}/^{218}\text{Ra}$	70	6	0.62	1.20	0.74	0.86
.....	90	8	0.58	1.16	0.67	0.82
$^{218}\text{Ra}/^{216}\text{Ra}$	73	6	0.68	1.20	0.81	0.9
.....	95	8	0.61	1.16	0.71	0.84

In the equation (5) we neglected a possible variation of the angular momentum within the two initial steps of the evaporation cascade and a small difference in the shapes and positions of the maxima of the excitation curves. We also assumed that the complete fusion cross section is reversely proportional to the center mass energy. To avoid the need of taking into account the influence of Coulomb barrier, we used in our calculations cross section data only for reactions with evaporation of $x \geq 6$ neutrons. Experimental values of $\frac{\sigma_{(x+2)n}}{\sigma_{xn}}$ as well as the deduced from these values reduced neutron widths are listed in Table 6. It is worth to remind that these cross-section ratios were measured in our experiments with an accuracy of $\pm 15\%$, and,

consequently, the deduced values of $\langle \Gamma_n / \Gamma_{tot} \rangle$ have the accuracy of $\pm(7-8)\%$. Taking this into account, one comes to the unequivocal conclusion that the result of calculations of $\langle \Gamma_n / \Gamma_{tot} \rangle$ values obtained with the parameter set (c) involving, in particular, the parameter value $\tilde{a}_f / \tilde{a}_\nu = 1.05$ are radically different from experimental points.

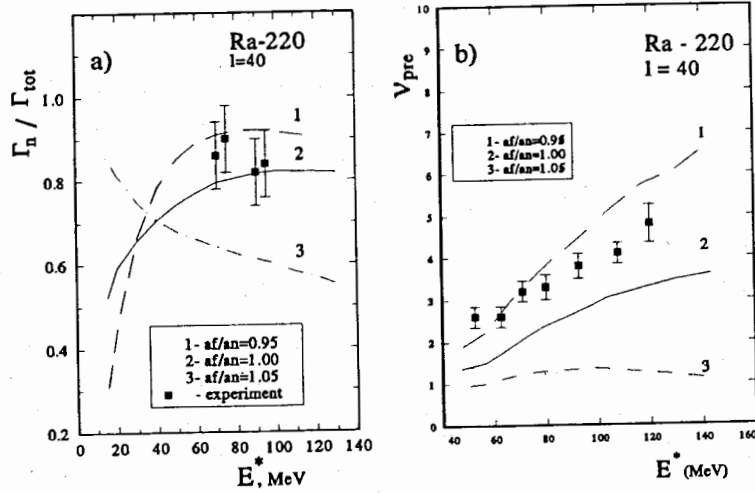


Fig. 3. a) Comparison of experimental and calculated mean reduced neutron width obtained for the compound nuclei of $^{218,220}\text{Ra}$. (See explanations in the text). b) Calculated numbers of pre-saddle neutrons obtained with different values of the parameter $\tilde{a}_f / \tilde{a}_\nu$. Symbols show the experimental pre-fission neutron numbers obtained in Ref. [30] for the compound nucleus of ^{213}Fr .

Therefore the parameter set (c) should be excluded from consideration, and we have a convincing experimental argument in favour of the use of only the range of $\tilde{a}_f / \tilde{a}_\nu \leq 1.00$.

The experimental values of $\langle \Gamma_n / \Gamma_{tot} \rangle$ also give the evidence that many steps of the de-excitation cascade contribute in the fission channel of the compound nuclei of $^{220,218,216}\text{Ra}$ having an initial excitation energy of $E^* = 80 - 90$ MeV. This observation correlates well with the results of our statistical model calculations.

The cross-section ratios measured for nuclei formed in the reac-

tions that involve different numbers of steps in the evaporation cascade allow us not only to experimentally limit the variation range for the parameter $\tilde{a}_f / \tilde{a}_\nu$ to the values of ≤ 1.00 , but also to estimate, on the basis of the experimental reduced widths $\langle \Gamma_n / \Gamma_{tot} \rangle$ obtained for initial steps of the evaporation cascade, the mean number of pre-saddle neutrons and compare this with the total number of pre-fission neutrons. To illuminate this point, we show in Fig.3b results of calculations for excitation energy dependence of the number of pre-saddle neutrons obtained with three different parameter sets (a, b and c).

Calculation of the number of neutrons evaporated before the compound nucleus reaches its saddle point gives (at the initial excitation energy of 100 MeV and integration made over the range of partial waves of $l \leq 40$) the values $\bar{\nu}_{pre}^{calc} = 3.0$ and $\bar{\nu}_{pre}^{calc} = 5.0$, respectively, at the parameter values $\tilde{a}_f / \tilde{a}_\nu$ equal to 1.00 and 0.95 (see Fig.3b). Solid squares in Fig.3b show the data of experiments [30] where the total number of pre-fission neutrons was obtained for the compound nucleus ^{213}Fr in dependence of its excitation energy. One can see that calculations using the parameter $\tilde{a}_f / \tilde{a}_\nu \leq 1.00$ give the results coinciding, or even exceeding, the experimental numbers of pre-fission neutrons. On a face of it, such a result of a statistical model calculation that is able to give the number of $\bar{\nu}_{pre}^{calc}$ surpassing the experimental value $\bar{\nu}_{pre}^f$ may appear peculiar. However, it is explained quite easy: partial waves of $l \leq 40$ contribute $\approx 30 - 40\%$ into the fusion reaction total cross section, therefore the main part of the cross section of the fusion-fission reaction is due to higher values of angular momentum. If one assumes that in experiments of the type described in Ref. [30] neutrons are detected in coincidence with fission fragments of compound nuclei having angular momentum values of up to l_{crit} , one should take into account all the partial waves up to $l_{crit} \cong 70$ in calculations made for Ra compound nuclei excited to ~ 100 MeV. In that case, calculations yield the $\bar{\nu}_{pre}^{calc}$ values of 1.8 and 2.8, respectively, with the $\tilde{a}_f / \tilde{a}_\nu = 1.00$ and 0.95. This implies that even in this case the part of pre-saddle neutrons makes from 50

to 80 % of the total number of pre-fission neutrons.

It is worth to add at this point that, when comparing with the experimental data, the employment of the complete set of partial waves extending up to l_{cr} might be not quite correct. The reason is that $\bar{\nu}_{pre}^f$ values were obtained in experiments where neutrons coinciding with fission fragments were detected. As a rule, detectors of fission fragments are placed at an angle close to 90° to the beam direction [31]. As it is well known, for $A \sim 200$ compound nuclei with the angular momentum of ~ 70 the fission fragment angular anisotropy makes ≥ 4 , and therefore, the contribution of larger partial waves in the observed fission events will be weakened at 90° . Hence, the real maximum angular momentum value in these experiments will be lower than l_{crit} . But, since the number of pre-saddle neutrons increases with the decrease of $\langle l \rangle$, one should take this into account, and this will result in a reduction of the difference obtained between the calculated and experimental values of $\bar{\nu}_{pre}^f$.

Finally, from the calculated widths estimations follow for the mean time that passes before ^{220}Ra compound nuclei with $l \leq 40$ achieve the saddle point. For example, at $l = 30$ and excitation energy of 100 and 80 MeV this time makes, respectively, $2.7 \cdot 10^{-20}$ and $3.6 \cdot 10^{-20}$ s, and these values are by one order of magnitude more than the mean times of neutron evaporation characteristic for such excitations.

5. Conclusion

Formation cross sections of evaporation residues have been measured for the reactions $^{22}Ne + ^{194,196,198}Pt$ in the range of 40 to 160 MeV of the compound nucleus excitation energy. These cross sections are well reproduced in the framework of the statistical model incorporating the Ignatyuk prescription for shell effects. The present results, together with those obtained in our previous studies [7-11, 23-26], showed that this model allows to correctly reproduce the cross sections of evaporation reactions in a wide range of compound nuclei extending from Bi to U.

Measurements of the cross-section ratios for individual reaction

products obtained as a result of evaporation cascades of different lengths allowed to estimate with a good accuracy the reduced neutron widths for compound nuclei at a high excitation energy. It was shown, by a comparison with calculations, that these cross-section ratios are extremely sensitive to the value of the parameter \bar{a}_f/\bar{a}_ν and, therefore, they allow to obtain this parameter value with a high degree of precision. Thus, testing calculation results with two sets of experimental data – the formation cross sections and cross-section ratios – permits to acquire independently the values of both principal parameters of the model – C and \bar{a}_f/\bar{a}_ν . Having at the disposal only the formation cross section of evaporation residues one could not disentangle these two parameters.

Having the parameter values of C and \bar{a}_f/\bar{a}_ν fixed, one can considerably enhance the reliability and accuracy of estimations of such values as the reduced fission width related to different stages of the evaporation cascade and number of pre-saddle neutrons, i.e the values that are not directly obtained in experiments. Our calculations showed that a considerable part of pre-fission neutrons (from 50 to 100 %) are pre-saddle. So, one can note that, for the studied compound nuclei having the excitation energy of up to ~ 160 MeV, statistical model calculations give the results that reproduce in a quite satisfactory way both, the decay widths and multiplicity of pre-fission neutrons.

The question arises: up to which excitation energy this model works and one can assume the complete fusion and fast compound nucleus equilibration to be the principal mechanism for formation of evaporation residues? We are planning to extend these experiments to the excitation energy of ~ 250 MeV with a hope that our separator technique will allow us to distinguish complete fusion reactions and accomplish the statistical model analysis of different de-excitation channels of compound nuclei.

This work was realized partly with the financial support of the International Science Foundation (grants RSV-300 and RSV-000) and Russian Basic Research Foundation (grants N96-02-17209 and N96-02-17209).

References

1. D.J.Hinde, Nucl.Phys. A553 (1993) 255.
2. D.Hilscher, H.Rossner, Ann. Phys. (Paris), 17 (1992) 471.
3. I.I.Gontchar, P.Frobrich, Nucl.Phys. A551 (1993) 495.
4. T.Wada, N.Carjan, Y.Abe, Nucl.Phys. A538 (1992) 283.
5. D.Ward, R.J.Charity, D.J.Hinde, J.R.Leigh, J.O.Newton, Nucl. Phys. A403 (1983) 189.
6. Yu.A.Muzychka, B.I.Pustyl'nik, Proc. Int. School-Seminar on HI Physics, JINR Report D7-83-664, Dubna, (1983) p.420.
7. D.D.Bogdanov, E.M.Kozulin, Yu.A.Muzychka, Yu.E.Penionzhkovich, B.I.Pustyl'nik, G.M. Ter-Akopian, Proc. Int. Workshop on Dynamical Aspects of Nucl.Fission, Smolenice, 1991, eds. J. Krisiak, B.I.Pustyl'nik (JINR Report E-92-95, Dubna, 1992) p.86.
8. G.M.Ter-Akopian, A.N.Andreyev, D.D.Bogdanov, V.I.Chepigin, A.P.Kabachenko, O.N. Malyshev, Yu.A. Muzichka, G.S. Popeko, B.I.Pustyl'nik, S.Sharo, R.N.Sagaidak, M.Veselsky, A.V. Yeremin, Nucl. Phys. A553 (1993) 735c.
9. A.N.Andreyev, D.D.Bogdanov, V.I.Chepigin, A.P.Kabachenko, O.N.Malyshev, Yu.A.Muzichka, B.I.Pustyl'nik, G.M. Ter-Akopian, A.V.Yeremin, Nucl.Phys. A568 (1994) 323.
10. A.N.Andreyev, D.D.Bogdanov, V.I.Chepigin, A.P.Kabachenko, O.N.Malyshev, Yu.A.Muzichka, Yu.Ts.Oganessian, A.G. Popeko, B.I.Pustyl'nik, J.Rohac, R.N.Sagaidak, A.V.Taranenko, G.M. Ter-Akopian, A.V.Yeremin, Nucl.Phys. A583 (1995) 153c.
11. A.N.Andreyev, D.D.Bogdanov, V.I.Chepigin, A.P.Kabachenko, O.N.Malyshev, Yu.A. Muzichka, Yu.Ts.Oganessian, A.G. Popeko, B.I.Pustyl'nik, J.Rohac, R.N.Sagaidak, A.V. Taranenko, G.M. Ter-Akopian, A.V.Yeremin, Proc. 7th Int. Conf. on Nucl. Reaction Mechanisms, Varenna, 1994, ed. E. Gadioli (Ricerca Scientifica ed Educazione Permanente Supplemento N.100. 1994) p.84.
12. A.V.Yeremin, A.N.Andreyev, D.D.Bogdanov, V.I.Chepigin, V.A.Gorshkov, A.V.Ivanenko, A.P.Kabachenko, L.A.Rubinskaya, E.M.Smirnova, S.V.Stepantsov, E.N.Voronkov, G.M. Ter-Akopian, Nucl.Inst.and Meth. A274 (1989) 528.
13. A.V.Yeremin, A.N.Andreyev, D.D.Bogdanov, V.I.Chepigin, V.A.Gorshkov, A.P.Kabachenko, O.N.Malyshev, A.G.Popeko, R.N.Sagaidak, S.Sharo, E.N.Voronkov, A.V.Taranenko, G. M. Ter-Akopian, A.Yu.Lavrentjev, Nucl. Inst.and Meth. A350 (1994) 608.
14. A.N.Andreyev, V.V.Bashevoy, D.D.Bogdanov, V.I.Chepigin, A.P.Kabachenko, O.N.Malyshev, J.Rohac, S.Sharo, A.V. Taranenko, G.M. Ter-Akopian, A.V.Yeremin, Nucl. Inst. and Meth. A364 (1995) 342.
15. A.H.Wapstra, G.Audi and R.Hoekstra, ADND Tables 39 (1988) 281.
16. W.Westmeier and A.Merklin, Phys. Date 29 (1985) 1.
17. A.V.Ignatyuk, G.N.Smirenkin and A.S.Tishin, Yad.Fiz. 21 (1975) 485.
18. S.Cohen, F.Plasil and W.J.Swiatecki, Ann.Phys. 82 (1974) 557.
19. C.M.Perey and F.G.Perey, ADND Tables 17 (1976) 2.
20. P.Frobrich, Phys. Rep. 116 (1984), 337.
21. A.V.Ignatyuk, G.N.Smirenkin, M.G.Itkis, S.I.Mulgin, V.N.Okolovich, Particles and Nuclei 16 (1985) 709.

22. J.O.Newton, *Particles and Nuclei* 21 (1990) 821.
23. A.N.Andreyev, D.D.Bogdanov, V.I.Chepigin, A.P.Kabachenko, Yu.A.Muzichka, O.A.Orlova, B.I.Pustyl'nik, S. Sharo, G. M. Ter-Akopian, A.V.Yeremin, *Yad.Fiz.* 52 (1990) 640.
24. A.N.Andreyev, D.D.Bogdanov, V.I.Chepigin, A.P.Kabachenko, Yu.A.Muzichka, O.A.Orlova, B.I.Pustyl'nik, S. Sharo, G.M.Ter-Akopian, A.V.Yeremin, *Proc.Int. School-Seminar on HI Physics, Dubna, 1989, (JINR Report D7-90-142, Dubna, 1990)* 499.
25. A.N.Andreyev, D.D.Bogdanov, V.I.Chepigin, A.P.Kabachenko, O.N.Malyshev, Yu.A.Muzichka, B.I.Pustyl'nik, R.N.Sagaidak, G.M.Ter-Akopian, A.V.Yeremin, *Yad.Fiz.* 58 (1995) 791.
26. A.N.Andreyev, D.D.Bogdanov, V.I.Chepigin, A.P.Kabachenko, O.N.Malyshev, Yu.A.Muzichka, A.G.Popeko, B.I.Pustyl'nik, J.Rohac, R.N.Sagaidak, A.V.Taranenko, G.M.Ter-Akopian, A.V.Yeremin, *Proc. Int. Workshop " Heavy-ion Fusion." Padova, Italy, 1994, eds. A.M. Stefanini et al. (World Scientific, Singapore 1994)* p.254.
27. A.J.Sierk, *Phys.Rev.* C33 (1986) 2039.
28. M.Blann, M.Beckerman, *Phys.Rev.* C17 (1978) 1615.
29. A.N.Andreyev, D.D.Bogdanov, S.Sharo, G.M.Ter-Akopian, M.Veselsky, A.V.Yeremin, *Phys.Lett.B* 312 (1993) 49.
30. D.J.Hinde, D.Hilscher, H.Rosner, B.Gebauer, M.Lehmann, M.Wilpert, *Phys.Rev.* C45 (1992) 1229.
31. D.J.Hinde, D.Hilscher and H.Rosner, *Nucl.Phys.* A502 (1992) 497.

Received by Publishing Department
on October 4, 1996.